JOURNAL OF APPLIED ELECTROCHEMISTRY 20 (1990) 798–803

Investigation of anodic aluminium oxide layers by electrochemical impedance spectroscopy

B. VAN DER LINDEN, H. TERRYN, J. VEREECKEN

Vrije Universiteit Brussel, Department of Metallurgy, Electrochemistry and Materials Science, Pleinlaan 2, B-1050 Brussels, Belgium

Received 4 December 1989

The effects of a.c.-electrochemical graining and anodizing of an aluminium substrate on the layer properties of both barrier and porous alumina layers are examined using electrochemical impedance spectroscopy (EIS). In order to show the capabilities of the technique for a quantitative determination, results based on impedance data are compared with complementary information from surface analytical techniques. Though the results for the determination of barrier layer thickness and dielectric constant look promising, calculations are troubled by non-trivial dispersion phenomena. This problem is treated using a fractal description of surface roughness of the substrate and of the layer thicknesses. Information on pore structure of porous oxide films could not be obtained from the approach considered in this study.

Nomenclature

C_b geometric barrier layer capacitance ($\mu F\,cm^{-2}$)
C_p porous layer capacitance
c_d elementary surface capacitance of the double layer
R_p resistance of the solution in pores ($\Omega\,m^{-2}$)
r_e elementary resistance of the solution near the surface
D_f fractal dimension of the surface
E_a anodizing voltage (V)
r_a unit barrier thickness ($nm\,V^{-1}$)
A_g geometric surface area (cm^2)
d_b thickness of the barrier layer (nm)
α fractional power frequency dependence
ω angular frequency of the a.c.-voltage ($rad\,s^{-1}$)
ε_0 permittivity of free space ($8.85 \times 10^{-12}\,F\,m^{-2}$)
ε dielectric constant of the anodic oxide
σ surface roughness factor
j unit on imaginary axis

impedances:

$Z = Z' - jZ''\ (\Omega\,m^{-2})$

1. Introduction

In the construction industry where electronic and lithographic applications are used, aluminium is submitted to a variety of surface treatments such as graining and anodizing. The graining process provides a rough surface topography of the substrate and results – for example, in an appropriate differentiation of ink-receptive image areas and water receptive non-image areas in offset-printing or, in the case of electrolytical capacitors – in a high capacitance per square centimetre geometric surface area. During anodizing an alumina layer is formed on the substrate which provides a much higher corrosion and abrasion resistance of coils or appropriate dielectric properties.

A survey of the literature shows that surface analytical techniques including scanning and transmission electron microscopy (SEM, TEM) and surface area measurements by gas adsorption were widely used to determine the layer properties. These techniques suffer from rather long specimen pretreatment and operation times. Therefore, electrochemical impedance spectroscopy (EIS) was proposed [1] for its capability as an on-line detection technique, due to its relatively good feasibility for specimen handling and data interpretation.

The interpretation of impedance data of anodic alumina films was generally considered in terms of macroscopic equivalent circuits. Early studies by Hoar and Wood [1] proposed, for sulphuric acid-anodized and sealed aluminium, a parallel equivalent for the barrier layer capacitance (C_b), and an impedance for the solution in the pores (R_p) and for the porous oxide film (C_p). This model was adopted by Mansfeld and Kendig [2] for the investigation of anodizing layers [3]. A second equivalent circuit was based on a series equivalent for C_b and the porous film (C_p and R_p) [4–6].

For unsealed porous films the impedance spectra mainly consisted of a barrier layer capacitance [2], due to the relatively small value of R_p, contributing a leakage path in parallel with the oxide cells. Considering the film as an ideally behaved capacitor or dielectric, the barrier layer thickness (d_b) could be determined

0021-891X/90 $03.00 + .12

[1, 6]. Under the same assumptions, the porous layer thickness could also be calculated [5] for partially sealed oxide films.

The impedance data obtained for solid electrodes showed a dispersion phenomenon, giving rise to a fractional power frequency dependence (fpfd) [1, 9]. These effects were interpreted in two ways. In the case of oxide films, the spreading of the relaxation times of polarization phenomena [6, 20] caused dispersion to appear in the Cole–Cole plot [21]. Richardson *et al.* [7] showed that there could be a considerable effect of flaws on the impedance characteristics, leading to dissipation factors, roughly invariant with frequency (10^2–10^5 Hz).

In the case of ideally polarizable electrodes, the presence of a fpfd could be related to the surface roughness. Experimental results [8–14] showed this should be due to the coupling of the elementary impedances of the double layer capcitance (C_d) and electrolyte resistance (r_e) at the surface. De Levie [8] and Scheider [9] described the dispersion phenomenon in terms of infinitely long, branched ladder–networks of c_d and r_e, different degrees of branching leading to different values of the fpfd α. Assuming the rough surface to be self-similar under scale transformation [15], Le Méhauté [10] and Nyikos *et al.* [11] developed a relation between α and the fractal dimension (D_f) of the surface [15]. Later, Liu *et al.* [13] and Keddam *et al.* [12] showed that a blocked, fractal electrode surface gives rise to fpfd, although the relation between α and D_f is not simple. Nevertheless it has been pointed out by many authors [10–15] that self-similarity is a less stringent assumption than of 'well-ordered surface irregularities' [8, 9].

The purpose of this study is to evaluate the capabilities of EIS for the determination of the layer properties resulting from various aluminium pretreatments and anodizing processes. The investigation is focused on the quantitative estimation of layer thicknesses, dielectric properties of the oxide(s), substrate roughness and, in the case of porous layers, pore size, cell volume and pore distribution [16].

For the interpretation and quantification, pretreatments and anodizing were performed under well-controlled conditions, giving rise to well-known oxide layers [16, 22]. Also, the EIS results were extensively checked against complementary results from surface examination techniques (SEM, TEM).

2. Experimental details

2.1. *Aluminium pretreatments*

The electrodes were prepared from cold rolled 99.5% (AA1050) aluminium alloy (0.29% wt Fe, 0.10% Si, 0.04% Cu, 0.002% Mn, 0.002% Ti, 0.003% Zn). All experiments were carried out in a 0.1 l vessel, thermostatically controlled to $\pm 0.5°$ C, in which an aluminium working and counter electrode and a calomel reference electrode were mounted.

In order to obtain samples with varying substrate roughness the following treatments were performed prior to anodizing: (i) degreasing (only) of the rolled aluminium; (ii) electropolishing, performed in a perchloric acid solution at a current density of 30–35 A dm^{-2}, a temperature of 15° C and for a period of 2 min; (iii) a.c.-electrograining was done in a stirred 0.1 M HCl solution at 40° C with a 15 A_{RMS} dm^{-2} current density, using a frequency of 50 Hz. The total graining time was 90 s. The morphology obtained after this treatment has been discussed in separate papers [16, 19].

Early observations revealed the formation of an adherent film of reaction products on the a.c.-grained electrode. Removal, without dissolution of the aluminium substrate, of this etch film was carried out in a boiling 0.2 M chromic – 0.55 M phosphoric acid solution.

2.2. *Anodizing conditions*

The pretreated Al-electrodes were anodized in two types of solution according to the desired oxide layer. Barrier oxide layers were formed in 3% tartaric acid solution at pH 5.5 (current density = 0.88 A dm^{-2}, T = 25° C). Anodic oxidation was interrupted at different potentials (10, 20 and 100 V). Porous oxide layers were formed in a 20% sulphuric acid or a 4% phosphoric acid solution at 22° C. The current density was varied in the range 0.25–4 A dm^{-2} in order to obtain various barrier layer thicknesses.

2.3. *Impedance measurements*

A.c.-impedance measurements were carried out on a specimen of 1.13 cm^2 geometric area. The test solution was a 0.2 M K_2SO_4-solution with pH adjusted to 5 and at T = 298 K. The cell consisted of a Hg/Hg_2Cl_2–KCl (sat.) reference electrode and a platinum wire counter electrode with high surface area. Experiments were carried out under potentiostatic control of a PAR 273-potentiostat, using the conventional three electrode configuration. The impedance spectra were recorded on a SOLARTRON 1250 frequency response analyzer. The d.c.-bias was chosen at −150 mV with respect to the calomel-reference, although this did not have any effect on the impedance data in the range −300 to +300 mV. Linearity of the current response was assured for a.c.-signal amplitudes between 10 and 100 mV_{RMS}. The amplitude chosen was 50 mV_{RMS}.

The solution resistance between the specimen and the reference electrode was eliminated from the impedance data by extrapolation of the series resistance to infinite frequency. Finally, to be sure that the measured impedances are characteristic only of the oxide film(s), the influence of the electrolyte concentration was checked for every series of specimens. For specific resistance of the K_2SO_4-solutions between 5.0 and 150 Ωm no effects of the solution (and the d.c.-potential) on the impedance data were observed. It could therefore be concluded that no contribution

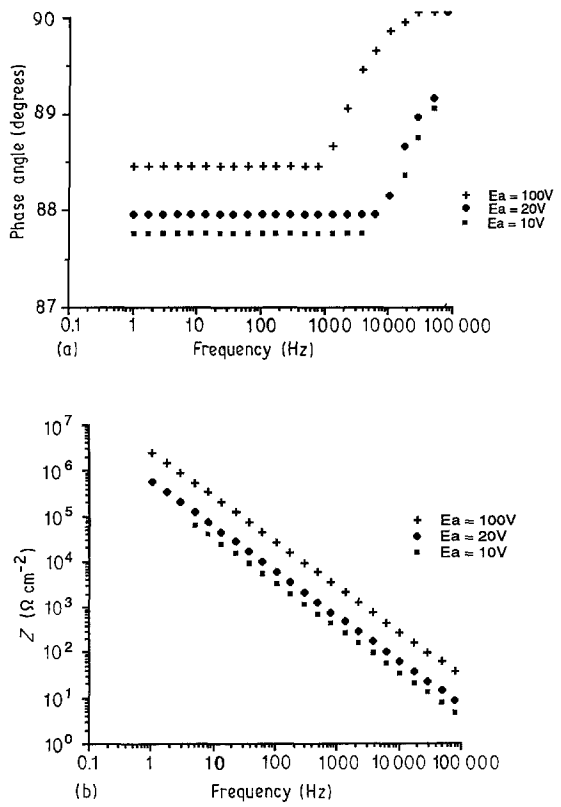

Fig. 1. Bode plots of the barrier layer impedance for different anodizing voltages E_a, in an ammonium tartrate electrolyte.

of the electrochemical double layer losses to the total impedance was found.

3. Results and discussion

3.1. *Barrier layers on rolled aluminium*

The quantitative determination of barrier-type anodic film properties (layer thickness, dielectric constant, substrate roughness) are of prime interest. Therefore ammonium tartrate was used as anodizing electrolyte at different anodic voltages (E_a). The layer thickness (d_b) can be calculated from the unit barrier thickness (r_a) according to the relation

$$d_b = r_a E_a \qquad (1)$$

with r_a in the range 1.1–1.3 nm V^{-1} for NH_4-tartrate according to [17]. In this investigation a value of 1.1 nm V^{-1} is retained (see above). The Bode plots of the impedances for anodic voltages between 10 and 100 V, are presented in Fig. 1. It can be seen that they do not indicate a purely capacitive impedance behaviour. A constant phase angle (c.p.a.) of about 88° instead of 90° appears for frequencies between 10° and 10^3 Hz (deflections at higher frequencies are introduced by the substraction of the solution resistance, predominating over the oxide film impedance). The empirical relation for the layer impedance can be written:

$$Z = 1/(j\omega)^{\alpha} C_b \qquad (2)$$

This corresponds to a frequency dispersion of the layer capacitance with a dissipation factor invariant

Table 1. Values for the CPA-element $Z = 1/(j\omega)^{\alpha} C_b$ as a function of the barrier layer thickness for different anodizing electrolytes: (a) ammonium tartrate, $r_a = 1.1\,nm\,V^{-1}$; (b) sulphuric acid, $r_a = 1.0\,nm\,V^{-1}$; (c) phosphoric acid, $r_a = 1.0\,nm\,V^{-1}$

	d_b (nm)	C_b (μF cm^{-2})	α
(a)	12.0	0.690	0.966
	24.0	0.357	0.985
	120.0	0.077	0.988
(b)	3.5	2.00	0.957
	5.7	1.19	0.969
	8.5	0.836	0.981
	12.0	0.585	0.985
(c)	18.0	0.368	0.989
	57.0	0.133	0.990
	85.0	0.090	0.990

with frequency. C_b is the (frequency-independent) barrier layer capacitance. The values of C_b and α can be calculated from the results of Fig. 1 (Table 1a) which show that α falls slightly with d_b. The values of C_b can be used to check for the familiar parallel-plate capacitor relationship:

$$C_b = \varepsilon\varepsilon_0 \frac{A_g}{d_b} \qquad (3)$$

Using Table 1a, the relation between C_b and d_b can be deduced and as shown in Fig. 2, this behaviour is linear on the log–log scale. From the ordinate at $d_b = 0$, a value of $\varepsilon = 8.5$ can be calculated, which agrees with values reported by other investigators [18].

Impedance data for samples (22.0 nm barrier film) with different geometric surface area (A_g) are presented in Fig. 3 and result in a linear variation of C_b with A_g (Equation 3). Other experiments show that this behaviour holds for a layer thickness between 11.0 and 110.0 nm. Using (3) with the impedance results for different A_g and taking $\varepsilon = 8.5$, it is now possible to verify the value of d_b. Table 2 reflects the differences between results from impedance measurements with varying A_g, using 1.1 nm V^{-1} as unit barrier thickness

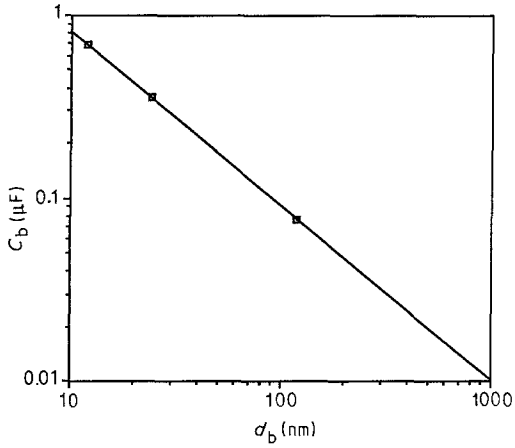

Fig. 2. Variation of the barrier layer capacitance with the barrier layer thickness for barrier layers formed in ammonium tartrate. The layer thickness is calculated using 1.1 nm V^{-1} as unit barrier thickness.

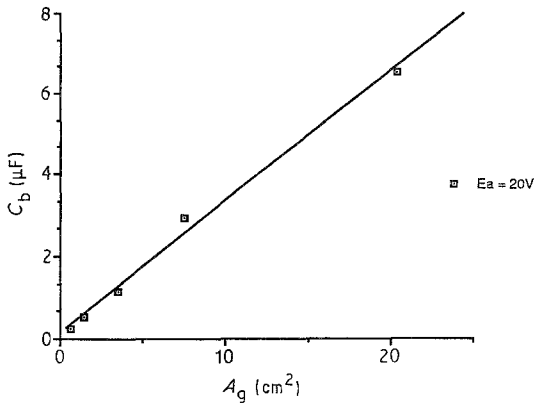

Fig. 3. Effects of the geometric surface area of the specimen on the capacitance of a 22.0 nm thick barrier layer formed in ammonium tartrate.

and values calculated from one-frequency measurement. It is clear from Table 2 that erratic results are obtained using latter measurements or ignoring the effects of dispersion.

3.2. *Effects of the substrate roughness*

Micrograph 1 shows the effects of a.c.-electrochemical graining on the substrate topography. It can be seen that graining causes a substantial increase of the surface area of the substrate. As the barrier layer follows the substrate topography [16, 17], the same conclusion can be drawn for the alumina surface.

In order to characterize this roughening process, impedance spectra of anodic oxide layers on differently treated Al-substrates are compared:

as-received or rolled Al;
electropolished;
a.c.-electrochemically grained.

In Fig. 4 the variation of C_b with the surface roughness is presented for three different anodizing voltages 10, 20 and 100 V. Electrochemical graining is seen to cause an increase of about 25% in C_b, relative to the electropolished samples, while the differences between electropolished and as-received ones are negligible. Further, impedance spectra show that the roughness has no effects on the value of the fpfd (Fig. 4).

Considering Equation 3, one may conclude that for very rough substrates a 25% increase in the surface area has to be taken into account. An additional parameter is needed to describe the influence of the true surface area. Yet, there is still no quantitative

Table 2. Comparison of values of the barrier layer thickness calculated from the CPA-element or from one-frequency-measurements at different frequencies (in Hz), taking α = 1

E_a (V)	CPA (nm)	IDEAL (nm)			
		10	100	1 k	10 k
10	12.3	12.0	12.4	12.8	13.3
20	23.7	21.6	22.2	22.7	23.2
100	120.0	96.4	98.9	101.0	104.0

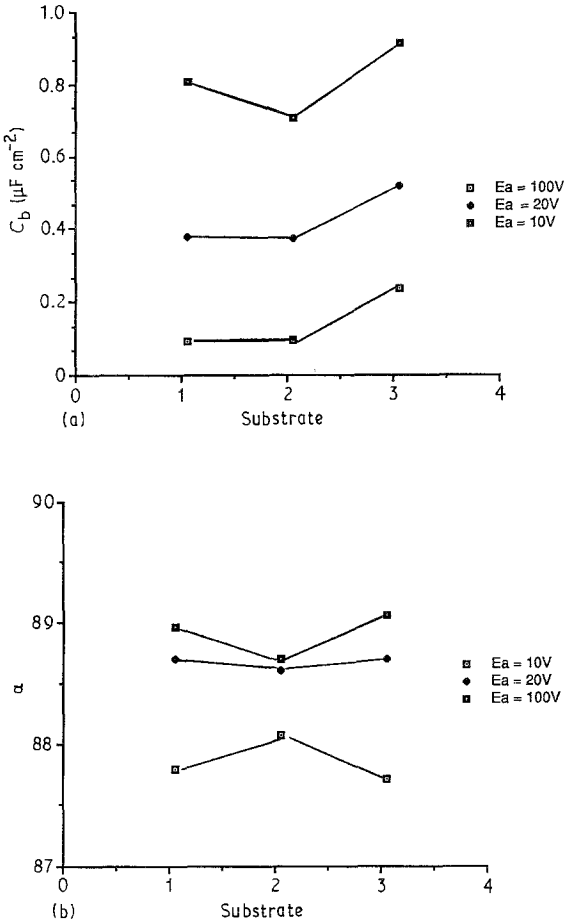

Fig. 4. Effects of the substrate roughness on C_b and the fpfd α for barrier oxide films (3% ammonium tartrate): 1 = electropolished; 2 = rolled, 3 = a.c.-electrograined.

relation found between the apparent increase in the substrate's surface area (Micrograph 1) and the impedance results. An adequate interpretation of EIS-results for layer properties (thickness, dielectric constant) after the anodizing process clearly needs a contribution for the substrate roughness.

3.3. *Porous oxide films on rolled aluminium*

In order to estimate the morphology (barrier and porous layer thickness, cell volume, pore size) of porous oxide layers formed during H_2SO_4 or H_3PO_4 anodizing, the latter properties are first determined [16] from SEM- and TEM-micrographs. In this case an anodizing ratio $r_a = 1.0\,\text{nm V}^{-1}$ is used [17] to calculate the barrier layer thickness.

Comparing the impedance spectra of a barrier oxide layer and a porous one with similar d_b (12.0 nm–roughly 1 μm pore thickness), no difference is observed (Fig. 5). For a 12.0 nm thick barrier layer, the presence of a porous oxide film does not contribute to the total impedance.

The effects of lowering the barrier layer thickness on the impedance spectra of porous oxides (Fig. 6a and b) can be handled in the same way as for barrier films (Table 1b and 1c). Figure 6 shows that the linearity (for a CPA-element) of the complex plane (Z', Z'') plot holds in a frequency domain between 10^{-1} and

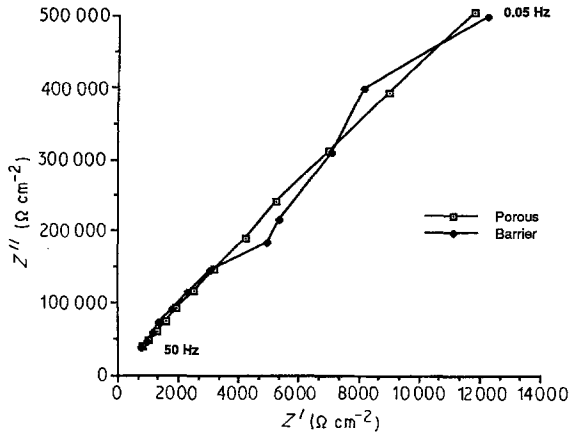

Fig. 5. Comparison of the impedance of a barrier (ammonium tartrate) and a porous (sulphuric acid) oxide layer, both with a barrier layer thickness of 12.0 nm.

10^2 Hz. The Nyquist representation is used for its higher sensitivity for changes in α.

In the case of sulphuric acid, α falls slightly with decreasing barrier layer thickness. This is probably due to the increasing importance of flaws for thin oxide films, giving rise to an additional dispersion effect [7]. Using $1.0\,\mathrm{nm\,V^{-1}}$ as unit barrier thickness for the calculation of d_b, the results of C_b (Table 1b

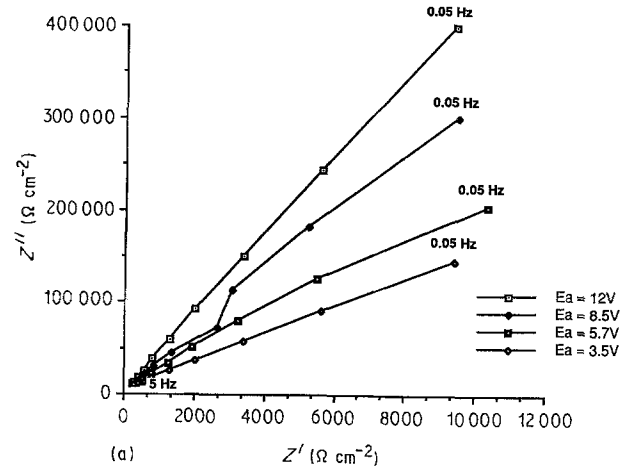

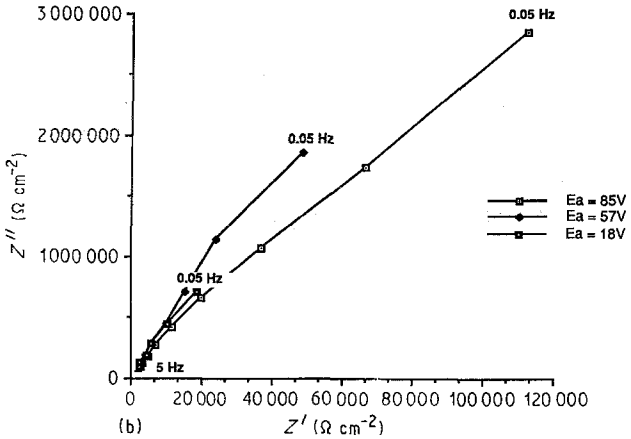

Fig. 6. Complex impedance plots (a) showing the CPA-behaviour of the barrier layer impedance and the decreasing fpfd with decreasing barrier layer thickness (porous anodizing in sulphuric acid – labels: frequency in Hz). (b) Complex impedance plots for phosphoric-acid-anodized Al-samples (labels: frequency in Hz).

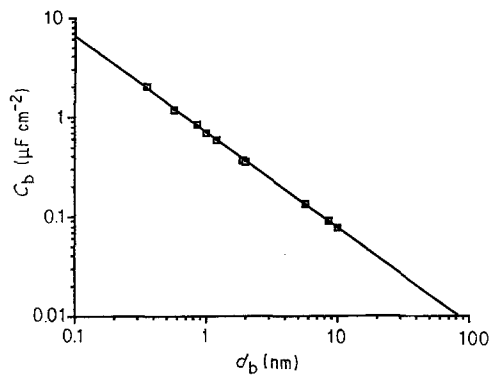

Fig. 7. Combined results from Table 1, showing the dependence of the barrier layer capacitance with the barrier layer thickness for both barrier and porous anodized samples.

and 1c) for porous films can be represented together with those from Table 1a for barrier films (Fig. 7). The linear behaviour indicates the consistency of taking $r_a = 1.1\,\mathrm{nm\,V^{-1}}$ for NH_4-tartrate.

It may be concluded that, concerning the barrier layer properties, the results obtained for barrier films are virtually identical to porous ones. Nevertheless, for porous oxide layers with thin barrier layers, the value of the dissipation factor is different for differing barrier layer thicknesses. This implies that in determining the barrier layer thickness from one-frequency measurement, erratic results are obtained. The error becomes more significant as the barrier layer thickness decreases. It is also clear that no information upon pore size, cell volume, cell thickness can be obtained directly from EIS.

3.4. *Proposed model*

It is obvious from these results that for quantitative estimation of layer properties from EIS, the effects of both frequency dispersion and substrate roughness have to be taken into account. According to Nyikos and Pajkossy [11] and Keddam *et al.* [12], dispersion phenomena can be related to surface roughness by the fractal description of the surface. In our study, a situation analogous to that observed for the coupling of the solution resistance and the double layer capacitance at ideally polarizable electrodes is occurring. The role of C_d is, in this case, played by the oxide layer capacitance showing fractal behaviour of the oxide film in both the surface area and thickness. Assuming, for example, a Cantor-bar model [13] for the oxide/solution interface, the basic relation between spatial scaling and frequency-dependence (given as Equation 8 in [11]) can be used to describe the effects of blowing up the system by a coefficient r. Therefore the barrier layer impedance can be calculated in the same way, using:

$$Z = \left(\sigma\varepsilon\varepsilon_0 \frac{A_g}{d_b}\rho^{1-\alpha}\right)^{-1} (j\omega)^{-\alpha} \qquad (4)$$

in which ρ represents the electrolyte specific resistivity and α is related to the fractal dimension of the surface

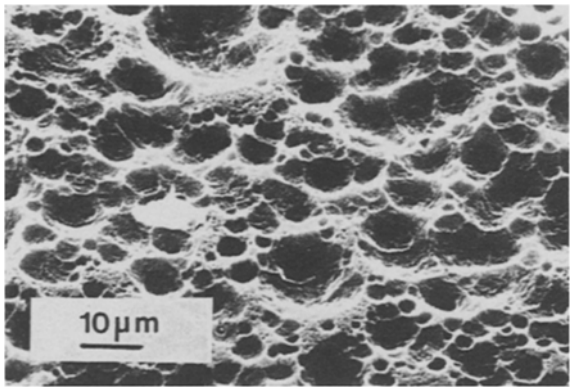

Fig. 8. Scanning electron micrograph of an a.c.-electrograined Al-substrate, showing a relatively high surface area due to the high density of hemispherical pits [16].

[11]. σ is to be interpreted as a dimensionless proportionality related to the (macroscopic) non-fractal surface roughness.

During the investigation, attempts were made, by changing the layer properties or the experimental conditions, to obtain values of the fpfd substantially different from the value of roughly 0.98, though no success was obtained in that direction. We therefore conclude that the fractal model of a metal/metal oxide/solution interface indeed provides a tool for determining quantitatively the layer thickness, though no further details of the microscopic irregularities can be obtained from the value of the fpfd.

If one considers the basic statement of Mandelbrot [15] about the need for using statistics or randomness for a practical relevance of fractal description of surface roughness, it is not surprising that model constructions [11, 12, 13] of fractal electrodes fail to link topography (D_f) with frequency-dependence (α). We therefore stress that a surface analytical determination of the Hurst-parameter [15] is needed for an accurate expression relating spatial irregularities and time-dependence.

4. Conclusion

This study has demonstrated the applicability of electrochemical impedance spectroscopy for quantitative determination of barrier layer properties (thickness, dielectric constant) of both barrier and porous oxide films. It is shown that measurements need to be taken over a wide frequency range to account for the influence of frequency dispersion of the layer capacitance. The dissipation factor α is found to be invariant with frequency.

The effects of the substrate roughness, due to a.c.-electrochemical graining, on the layer capacitance are not in complete accordance with results from electron micrographs. Only a 25% increase in C_b is found for an extremely rough surface.

The phenomena of dispersion and roughness are interpreted in terms of a fractal behaviour of layer surface and thickness, leading to two corresponding empirical constants.

It is finally shown that the presence of a porous oxide film has no influence on the impedance spectra. Further efforts are needed to determine the morphology and the porosity of these layers, using EIS.

References

[1] T. P. Hoar and G. C. Wood, *Electrochim. Acta* **7** (1962) 333.
[2] F. Mansfeld and M. W. Kendig, *Materials Science Forum* **8** (1986) in 'Electrochemical Methods in Corrosion Research', (edited by M. Duprat), Transtech Publications Ltd, Switzerland.
[3] *Idem, J. Electrochem. Soc.* **135** (1988) 828.
[4] M. Koda, H. Takahashi and N. Nagayama, International Society of Electrochemistry, Extended Abstracts of the 34th Meeting, Erlangen (1983) no. 0803.
[5] J. Hitzig, K. Jüttner, W. J. Lorenz and W. Paatch, *J. Electrochem. Soc.* **133** (1986) 887.
[6] R. Srinivasan and C. S. C. Bose, *J. Appl. Electrochem.* **12** (1982) 487.
[7] J. A. Richardson and G. C. Wood, W. H. Sutton, *Thin Solid Films* **16** (1976) 99.
[8] R. de Levie, *Electrochim. Acta* **9** (1964) 1231.
[9] W. Scheider, *J. Phys. Chem.* **79** (1975) 127.
[10] A. le Méhauté and G. Crépy, *Solid State Ionics* **9–10** (1983) 17.
[11] L. Nyikos and T. Pajkossy, *Electrochim. Acta* **30** (1985) 1533.
[12] M. Keddam and H. Takenouti, *ibid.* **33** (1988) 445.
[13] S. H. Liu, *Phys. Rev. Lett.* **55** (1985) 529.
[14] W. H. Mulder and J. H. Sluyters, *Electrochim. Acta* **33** (1988) 305.
[15] B. B. Mandelbrot, 'The Fractal Geometry of Nature', Freeman, San Francisco (1982).
[16] H. Terryn, PhD Thesis, Vrije Universiteit Brussel, Belgium (1987).
[17] S. Wernick, R. Pinner and P. G. Sheasby, 'The Surface Treatment and Finishing of Aluminium and its Alloys', 5th ed., vol. 1, Finishing Publication, Teddington, U.K. (1986).
[18] *ibid.* vol. 2.
[19] H. Terryn, J. Vereecker and G. E. Thompson, *Trans. Inst. Metal Finish* **66** (1988) 116.
[20] H. Birey, *J. Appl. Phys.* **49** (1978) 2898.
[21] K. S. Cole and R. H. Cole, *J. Chem. Phys.* **9** (1941) 341.
[22] H. Terryn, J. Vereecken, J. Vanhellemont and J. Van Landuyt, The Institute of Metal Finishing, Proc. Annual Technical Conference and Exhibition, Brighton, England (1989), 135.
[23] *Idem*, The Electrochemical Society, Proc. Symposium on Aluminium Surface Treatment Technology, ed. F. Alwitt, vol. 86 (1986), 291.